JOURNAL OF SOLID STATE CHEMISTRY **124,** 214–219 (1996)
ARTICLE NO. 0228

# Continuous Order–Disorder Transition in $Li_3Ni_2NbO_6$ and Cr-Doped $Li_3Ni_2NbO_6$ Rock Salt Structures

Glenn C. Mather and Anthony R. West

*Department of Chemistry, University of Aberdeen, Meston Walk, Aberdeen AB9 2UE, United Kingdom*

Received October 6, 1995; in revised form March 18, 1996; accepted March 21, 1996

**$Li_3Ni_2NbO_6$ has a partially ordered rock salt superstructure in which Nb occupies fully one set of octahedral sites and Li/Ni are distributed nonrandomly over three other sets of octahedral sites (Mather *et al.*, *J. Mater. Chem.* 5, 1177 (1995)). Over the temperature range 25–1100°C the Li/Ni site occupancy distribution is largely unchanged. Above 1100°C, Nb increasingly occupies the Li/Ni sites until, above 1300°C, the cations are completely disordered. The transition appears to be fully continuous, with no evidence of a transition enthalpy by DTA. $Cr^{3+}$ ions are able to substitute partially into both ordered and disordered structures by a range of mechanisms. The temperature range of the order–disorder transition decreases with Cr content, as shown in the phase diagram of the vacancy solid solutions, $Li_{3-x}Ni_{2-x}Cr_xNbO_6$ ($0 < x < 0.18$). The materials are modest semiconductors.** 

## INTRODUCTION

In the field of rock salt superstructure phases, the recently discovered family, $Li_3M_2XO_6$ ($M$ = Mg, Co, Ni; $X$ = Nb, Ta, Sb) is most unusual in showing a partial order of the cations (1, 2). The high valency $X$ atoms occupy fully one set of octahedral sites, but the Li and $M$ atoms are distributed in a nonrandom manner over three other sets of octahedral sites. The detailed occupancy pattern of these sites varies with $M$ and $X$ and, for a given $M$, $X$ was found to be essentially independent of the sample preparation procedure (2). Nevertheless, the possibility exists that the state of partial order of the Li/$M$ cations could be varied, perhaps as a function of temperature, as shown by the observation that the phase with $M$ = Co, $X$ = Nb has a simple cubic, fully disordered rock salt structure (2). In order to investigate further the possibility of structural changes at high temperature, we have investigated the properties of $Li_3Ni_2NbO_6$; these results are reported here. As well as using temperature to induce disorder, cationic substitutions may have a similar effect in cases where the substituting ions are able to occupy various sites in the host structure. To this end, the effect of substitutional Cr has been investigated, along with the effect on the electrical properties of introducing cation vacancies into the structures.

## EXPERIMENTAL

Samples were synthesized from $Li_2CO_3$ and oxides of the other components in appropriate ratios. The reagents were mixed in an agate mortar, using acetone to form a paste, dried, and fired in Pt boats in air. Initial firing was at 600–700°C to allow decarbonation to take place with a final firing at 1100°C for 48 h; samples were then cooled rapidly in air. In order to investigate possible structural changes in $Li_3Ni_2NbO_6$ with temperature, small samples were either slow-cooled from 1100°C at a rate of 1° $min^{-1}$ or quenched into Hg from temperatures in the range 1100–1300°C. For phase diagram determination on the join of general formula, $Li_{3-x}Ni_{2-x}Cr_xNbO_6$, pre-reacted samples were pelleted, heated at 800°C for 48 h, and then heated for short periods of time at 50° intervals in the range 800–1300°C. Samples were quenched in air or, for the higher temperatures, into Hg. Heating times at 1100°C and above were limited to about 10 min in order to prevent possible lithia loss by volatilization.

A Philips Hagg–Guinier X-ray powder diffraction camera was used to check phase purity. For accurate lattice parameter determination and Rietveld refinement, data were collected with a Stoe STADI P diffractometer, Cu$K\alpha_1$ radiation, with a small linear position sensitive detector. Unit cell parameters were obtained from data collected in the range $10° < 2\theta < 80°$ with Si as internal standard. For Rietveld refinement, a step width of 0.02° was used over the range $10° < 2\theta < 110°$ with a total collection time of about 12 h.

Elemental analysis was carried out on a Cameca SX51 electron probe microanalyzer, EPMA with standards of $LiNbO_3$ (for Nb and O), $FeCr_2O_4$ (for Cr), and Ni metal; Li could not be determined directly by EPMA. Conductivities of sintered pellets with Au electrodes were determined by standard two-terminal *ac* impedance measurements using Hewlett Packard 4192 and Solartron 1250/1286 instrumentation over the frequency range 30 mHz to 1 MHz.



0022-4596/96 $18.00

Differential thermal analysis, DTA, was carried out on a Stanton Redcroft 675 instrument over the temperature range 25–1300°C (heating rate 8°C $min^{-1}$).

Atomic coordinates are listed in Table 1 for samples with a range of thermal histories. The $R$ values are regarded as acceptable, taking into account the fact that the $R_{exp}$ values are artificially low as a consequence of limitations in the Stoe refinement package which did not permit constraints over the total occupancy for a particular cation over a number of sites; this led to an increase in the number of refined parameters and an artificially low $R_{exp}$.

## RESULTS AND DISCUSSION

### *Polymorphism of $Li_3Ni_2NbO_6$*

As a result of a range of experiments, detailed next, it has been shown that $Li_3Ni_2NbO_6$ undergoes a continuous order–disorder transition over the approximate temperature range 1100–1300°C. Below 1100°C, an equilibrium state of partial cation order occurs and it appears not possible to readily attain a state of complete cation order; above 1300°C, the cations are fully disordered; over the range 1100–1300°C, increasing cation disorder with increasing temperature occurs.

Rietveld refinement of powder X-ray data was carried out on a range of samples which had been heated isothermally at temperatures in the range 1100–1300°C followed by cooling at various rates. Results are summarized in Table 1 for six different thermal histories. Key points are as follows:

• For temperatures up to 1250°C, the XRD data were fully indexed on an orthorhombic unit cell, space group *Fddd*. On quenching from ≥ 1300°C, however, the structure was indexed on a cubic unit cell, space group *Fm3m*. The relationship between the two unit cells is $a_o = \sqrt{2}a_c$, $b_o = 2a_c$, $c_o = 3\sqrt{2}a_c$.

• The cell parameters vary significantly with thermal history, as shown in Fig. 1 for five different quench temperatures; data for 1100–1250°C are presented as pseudocubic parameters to facilitate comparison and to demonstrate how the distortion from cubic geometry decreases with temperature. Also shown are data for 1100°C but with a slower cooling rate. The data for quenched samples show a gradual, but increasingly rapid change in lattice parameters with increasing temperature, culminating in the completion of the transition to cubic symmetry by 1300°C. Thus, $a$ and $c$ increase with temperature, whereas $b$ decreases; the cell volume is essentially unchanged.

All the Hg-quenched samples exhibit larger lattice parameters, and larger cell volume, than those cooled more slowly from 1100°C. This is probably because these quenched samples contain considerable strains at room temperature, associated with the nonequilibrium excess of cation disorder brought about by their high temperature treatments. Thus, following Hauck (3), with increasing disorder there are more cation–cation repulsions between highly charged nearest cation neighbors, leading to a greater molar volume. On slower cooling, the stresses are relieved as the cations order into their equilibrium states and consequently, the unit cell contracts.

• The only significant differences in the refined atomic coordinates of the five orthorhombic samples, Table 1, concern the occupancies of the cation sites. The Nb site is fully occupied by Nb on quenching or slow cooling from 1100°C but gradually becomes a mixed cation site at 1200 and 1250°C. There is some limited evidence that the occupancies of the three sets of Li/Ni sites at 1100°C may change with cooling rate: for the Hg-quenched sample, the average occupancies of the three Li/Ni sites are slightly closer to the statistical 3:2 ratios, Table 1, than for the more slowly cooled samples. This is consistent with the observation that unit cell parameters on samples heated at 1100°C depend on cooling rate.

A full analysis, using the available software, of the occupancies of the cation sites for samples quenched from 1200 and 1250°C was not possible due to the presence of three cations in the various sites. The assumption was therefore made that, at these temperatures, the Li/Ni contents of each site were in the statistical ratio 3:2; there is some evidence of a trend toward statistical occupancy of the Li/Ni sites at 1100°C and this trend is expected to increase with temperature. It is concluded from the Rietveld refinements, therefore, that the first signs of an order–disorder transition are detected at 1100°C, by small variations in the Li/Ni site occupancies; major changes in site occupancies are seen at 1200 and 1250°C and the transition is complete by 1300°C. At 1300°C, the cation site occupancies are entirely statistical.

The progress of the transition may be seen in the temperature dependence of the Nb site occupancy, Fig. 2. The transition appears to be fully continuous and therefore, second order as also indicated by the lattice parameter data, Fig. 1. This is further supported by DTA results which showed no evidence of a phase transition in this temperature range, on either heating or cooling cycles. Consequently, there is no evidence for an enthalpy change, which could have indicated some first order character in the transition. Second order transitions involving the disordering of rock salt superstructures have been seen previously (4) in solid solutions between $Li_2TiO_3$ and MgO for a range of compositions containing ≥25% MgO. The transition temperature has not been determined directly. It is clearly somewhere between 1250 and 1300°C and, from the temperature dependence of the Nb 8(*a*) site occupancy over the range 1100–1250°C and its extrapolation to higher temperatures, the transition temperature is estimated to be close to 1300°C, as shown.

**TABLE 1**
**Structure Refinement Parameters for $Li_3Ni_2NbO_6$**

| Atom | Site | $x/a$ | $y/b$ | $c/z$ | $U_{iso}$ | Occupancy |
|---|---|---|---|---|---|---|
| | | (a) Slow-cooled in air at 1° $min^{-1}$ from 1100°C | | | | |
| | | *Fddd*; $a$ = 5.9067(4), $b$ = 8.4047(4), $c$ = 17.752(1) Å | | | | |
| Li(1)/Ni(1) | 16*g* | 1/8 | 1/8 | 0.2927(6) | 0.005 | 0.569(8)/0.431(8) |
| Li(2)/Ni(2) | 16*g* | 1/8 | 5/8 | 0.2867(6) | 0.005 | 0.586(8)/0.414(8) |
| Li(3)/Ni(3) | 8*b* | 1/8 | 5/8 | 1/8 | 0.005 | 0.65(1)/0.35(1) |
| Nb | 8*a* | 1/8 | 1/8 | 1/8 | 0.0011 | 1.00 |
| O(1) | 16*f* | 1/8 | 0.361(2) | 1/8 | 0.011(5) | 1.00 |
| O(2) | 32*h* | 0.115(2) | 0.377(2) | 0.2961(8) | 0.011(3) | 1.00 |
| | | $R_p$ = 7.66, $R_{wp}$ = 10.54, $R_I$ = 8.65, $R_{exp}$ = 4.9 | | | | |
| | | (b) Quenched in air from 1100°C | | | | |
| | | *Fddd*; $a$ = 5.9069(4), $b$ = 8.4012(4), $c$ = 17.750(1) Å | | | | |
| Li(1)/Ni(1) | 16*g* | 1/8 | 1/8 | 0.2930(5) | 0.001 | 0.561(7)/0.439(7) |
| Li(2)/Ni(2) | 16*g* | 1/8 | 5/8 | 0.2877(6) | 0.001 | 0.587(7)/0.413(7) |
| Li(3)/Ni(3) | 8*b* | 1/8 | 5/8 | 1/8 | 0.001 | 0.65(1)/0.35(1) |
| Nb | 8*a* | 1/8 | 1/8 | 1/8 | 0.007(1) | 1.00 |
| O(1) | 16*f* | 1/8 | 0.361(2) | 1/8 | 0.008(1) | 1.00 |
| O(2) | 32*h* | 0.114(2) | 0.376(1) | 0.2953(7) | 0.008(3) | 1.00 |
| | | $R_p$ = 7.28, $R_{wp}$ = 10.35, $R_I$ = 5.69, $R_{exp}$ = 5.2% | | | | |
| | | (c) Quenched in Hg from 1100°C | | | | |
| | | *Fddd*; $a$ = 5.9150(4), $b$ = 8.4072(4), $c$ = 17.767(1) Å | | | | |
| Li(1)/Ni(1) | 16*g* | 1/8 | 1/8 | 0.2926(5) | 0.001 | 0.555(7)/0.445(7) |
| Li(2)/Ni(2) | 16*g* | 1/8 | 5/8 | 0.2878(5) | 0.001 | 0.568(8)/0.432(8) |
| Li(3)/Ni(3) | 8*b* | 1/8 | 5/8 | 1/8 | 0.001 | 0.62(1)/0.38(1) |
| Nb | 8*a* | 1/8 | 1/8 | 1/8 | 0.005(1) | 1.00 |
| O(1) | 16*f* | 1/8 | 0.361(2) | 1/8 | 0.002(4) | 1.00 |
| O(2) | 32*h* | 0.114(2) | 0.377(1) | 0.2958(7) | 0.005(3) | 1.00 |
| | | $R_p$ = 8.10, $R_{wp}$ = 10.29, $R_I$ = 7.46, $R_{exp}$ = 1.13% | | | | |
| | | (d) Quenched in Hg from 1200°C | | | | |
| | | *Fddd*; $a$ = 5.9157(5), $b$ = 8.4033(5), $c$ = 17.777(1) Å | | | | |
| LiNi(1)/Nb(1) | 16*g* | 1/8 | 1/8 | 0.2925(7) | 0.021(4) | 0.96(1)/0.04(1) |
| LiNi(2)/Nb(2) | 16*g* | 1/8 | 5/8 | 0.2887(7) | 0.020(4) | 0.98(1)/0.02(1) |
| LiNi(3)/Nb(3) | 8*b* | 1/8 | 5/8 | 1/8 | 0.025(6) | 1.00/0.00 |
| LiNi(4)/Nb(4) | 8*a* | 1/8 | 1/8 | 1/8 | 0.014(2) | 0.15(3)/0.85(3) |
| O(1) | 16*f* | 1/8 | 0.364(3) | 1/8 | 0.014(4) | 1.00 |
| O(2) | 32*h* | 0.115(2) | 0.377(2) | 0.295(1) | 0.014(4) | 1.00 |
| | | $R_p$ = 9.41%, $R_{wp}$ = 12.06%, $R_I$ = 8.48%, $R_{exp}$ = 1.12% | | | | |
| | | (e) Quenched in Hg from 1250°C | | | | |
| | | *Fddd*; $a$ = 5.9199(5), $b$ = 8.3939(5), $c$ = 17.780(1) Å | | | | |
| LiNi(1)/Nb(1) | 16*g* | 1/8 | 1/8 | 0.2928(8) | 0.020(4) | 0.91(2)/0.09(2) |
| LiNi(2)/Nb(2) | 16*g* | 1/8 | 5/8 | 0.2905(8) | 0.021(4) | 0.92(2)/0.08(2) |
| LiNi(3)/Nb(3) | 8*b* | 1/8 | 5/8 | 1/8 | 0.025(7) | 0.95(2)/0.05(2) |
| LiNi(4)/Nb(4) | 8*a* | 1/8 | 1/8 | 1/8 | 0.019(3) | 0.29(4)/0.71(4) |
| O(1) | 16*f* | 1/8 | 0.368(3) | 1/8 | 0.015(5) | 1.00 |
| O(2) | 32*h* | 0.117(3) | 0.376(2) | 0.294(1) | 0.015(5) | 1.00 |
| | | $R_p$ = 9.47, $R_{wp}$ = 12.99, $R_I$ = 9.12, $R_{exp}$ = 1.12% | | | | |
| | | (f) Quenched in Hg from 1300°C | | | | |
| | | *Fm*3*m*; $a$ = 4.1915(1) Å | | | | |
| LiNi(1)/Nb(1) | 4*a* | 0 | 0 | 0 | 0.012(1) | 0.8333/0.1667 |
| O(1) | 4*b* | 1/2 | 1/2 | 1/2 | 0.010(1) | 1.00 |
| | | $R_p$ = 7.12, $R_{wp}$ = 9.53, $R_I$ = 2.79, $R_{exp}$ = 1.24% | | | | |

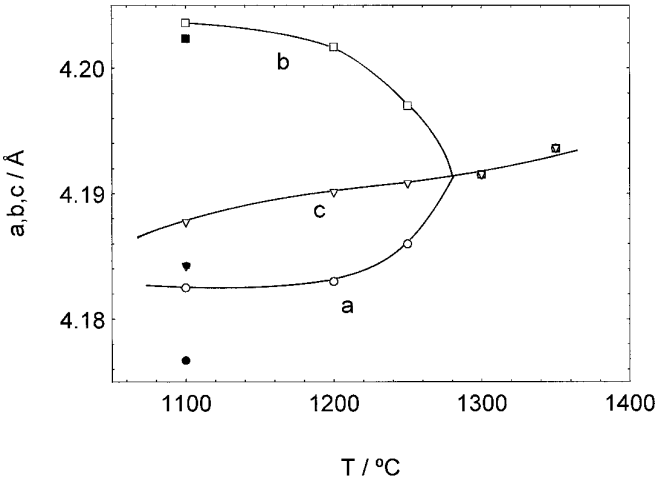


**FIG. 1.** Lattice parameters, at room temperature, of samples heated isothermally at various temperatures. Open data points, samples quenched into Hg; closed data points, samples slow-cooled in the furnace.

**TABLE 2**
**Unit Cell Parameters for Various Cr-Doped $Li_3Ni_2NbO_6$ Solid Solutions**

| Composition | Structure | Cell parameters(Å) | Volume per rock salt unit (Å$^3$) |
|---|---|---|---|
| | | $Li_3Ni_{2-3x}Cr_{2x}NbO_6$ | |
| $x = 0.1$ | disordered rock salt | $a = 4.1865(2)$ | 73.30 |
| $x = 0.2$ | disordered rock salt | $a = 4.1852(3)$ | 72.23 |
| | | $Li_{3-x}Ni_2Cr_{2x}Nb_{1-x}O_6$ | |
| $x = 0.1$ | ordered rock salt | $a = 5.903(2)$ | 72.68 |
| | | $b = 8.393(3)$ | |
| | | $c = 17.718(7)$ | |
| $x = 0.2$ | disordered rock salt | $a = 4.1777(5)$ | 72.84 |
| | | $Li_3Ni_{2-2x}Cr_{3x}Nb_{1-x}O_6$ | |
| $x = 0.1$ | disordered rock salt | $a = 4.1816(4)$ | 73.05 |
| $x = 0.2$ | disordered rock salt | $a = 4.1728(5)$ | 72.59 |

### *Cr-Doped $Li_3Ni_2NbO_6$*

In parallel with the study of the temperature dependence of the structure of $Li_3Ni_2NbO_6$, the effect of addition of $Cr^{3+}$ was investigated; $Cr^{3+}$ was chosen as a cation similar in size to Li, Ni, and Nb which could, in principle, substitute for any or all three of these cations in the crystal structure. Several compositions were prepared and reacted to investigate a range of possible solid solution mechanisms. It was found that $Li_3Ni_2NbO_6$ is indeed a versatile structure for doping as summarized in Table 2 for three different mechanisms and in Fig. 3 for a fourth mechanism. Three of these mechanisms necessitate cation vacancy creation to maintain charge balance and in one, the total cation content stays unchanged. Depending on the mechanism, the products either retain the ordered orthorhombic structure or adopt the cubic rock salt structure with complete cation disorder.

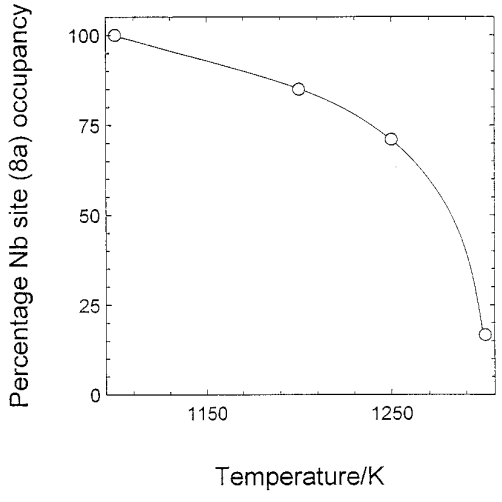


**FIG. 2.** Nb site occupancy as a function of annealing temperature.

A more detailed study of the mechanism Li + Ni $\Rightarrow$ Cr was made by determining the phase diagram for solid solutions of the general formula $Li_{3-x}Ni_{2-x}Cr_xNbO_6$. The phase diagram was determined as follows. Data were collected for samples of different composition $x$ on the Stoe diffractometer in the range $40° \leq 2\theta \leq 50°$. This region was chosen since it contains the most intense reflections from the ordered cell (2 0 6) and subcell (0 4 0) lines. These reflections were deconvoluted using a Pearson VII profile shape function using the program FIT (Stoe software). From the relative integrated intensities of the two reflections, it was possible to investigate whether particular samples were ordered, partially ordered or completely disordered. Figure 4 shows the change in relative intensities of the (206) and (040) reflections of the ordered cell on quenching a sample of composition $x = 0.175$ from temperatures of 900, 1000, and 1100°C. Once disordering is complete, the (206) reflection is no longer observed and the pattern can be indexed on a cubic unit cell, in which case the (040) reflection is reindexed as the (020) reflection of the cubic cell.

The phase diagram results are presented in Fig. 3. They show an extensive range of solid solution formation in both low temperature orthorhombic and high temperature cubic polymorphs with a phase transition zone that is clearly 200–300°C wide for all compositions. The temperature range of the phase transition moves gradually to lower temperatures with $x$ which is consistent with the increased cationic disorder that is inevitable on introducing a third cation, $Cr^{3+}$, onto the Li/Ni cation sites that already show considerable disorder.

In order to confirm that the transitional region in Fig.

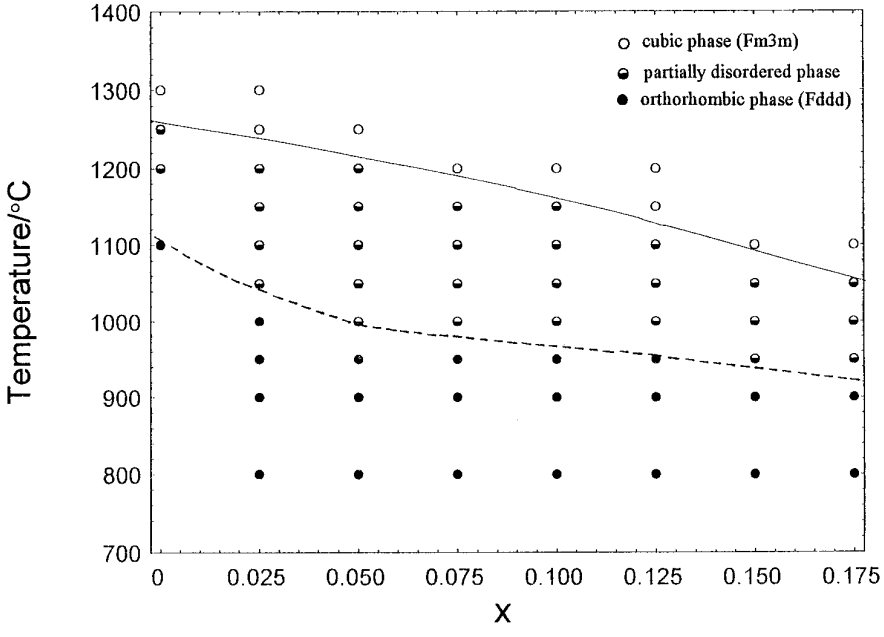


**FIG. 3.** Phase diagram of the solid solution system $Li_{3-x}Ni_{2-x}Cr_xNbO_6$ showing the order–disorder transition zone.

3 involved a progressive transformation of homogeneous material, rather than the break-up into a classical two-phase region, EPMA measurements were made on pellet fragments of one composition, $x = 0.15$, that had been heated isothermally for several hours at 800, 1000, 1100, and 1200°C, respectively. In all cases, back scattered electron images showed that the samples were single phase at the micrometer level, thus supporting the continuous nature of the transition.

The conductivity of three pellets of composition $x = 0.05$, 0.10, 0.15 was measured over the range 25–400°C. *ac* impedance plots showed rather broad arcs with low associated capacitance, ~10–20 pF $cm^{-1}$, that was attributed to the bulk response of poorly sintered ceramics.

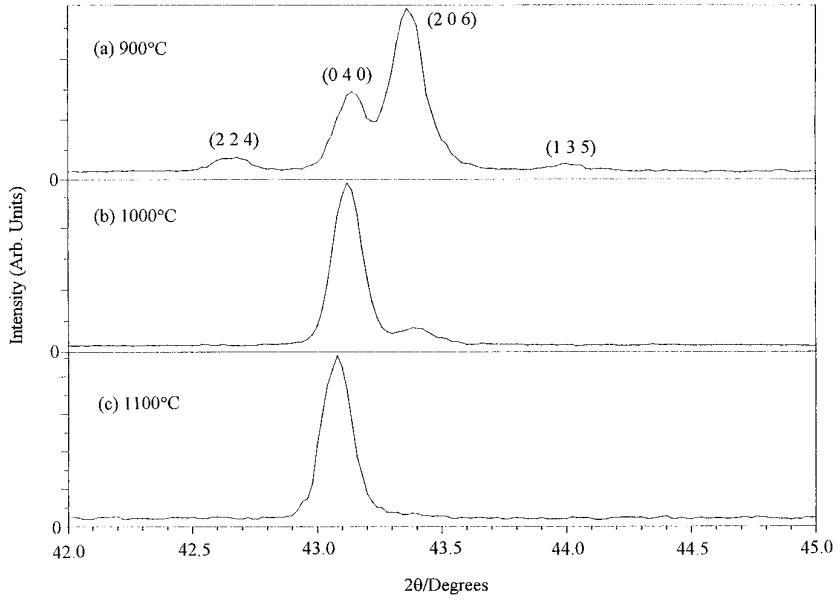


**FIG. 4.** Change in relative intensities of 040 (subcell) and 206 (supercell) reflections for $x = 0.175$ as a function of annealing temperature. The intensity of the 206 reflection provides an indication of the degree of cation order.

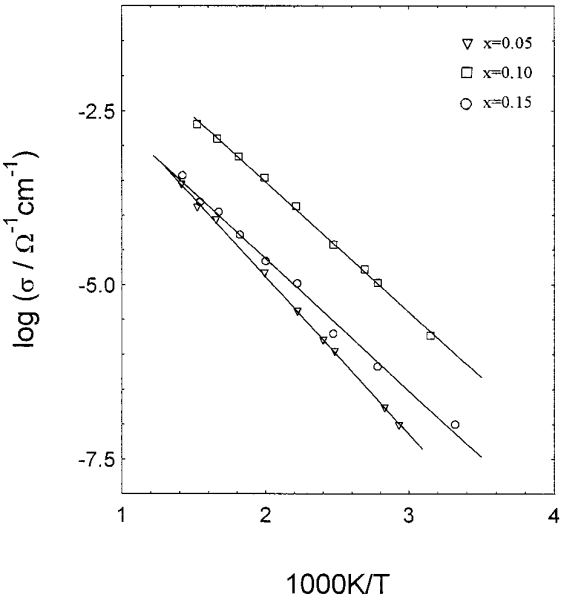


**FIG. 5.** Conductivity Arrhenius plots for three compositions.

Resistance values were obtained from the low frequency intercepts on the real, $Z'$ axis; these correspond approximately to the bulk resistance of the samples. These are presented as conductivity Arrhenius plots in Fig. 5. The conducting species is almost certainly electronic since the impedance complex plane plots showed no evidence of a low frequency ''electrode spike'' which, if observed could be attributed to the polarization of mobile $Li^+$ ions at the blocking Au electrodes. Hence, in spite of the significant concentration of cation vacancies, there is no evidence of $Li^+$ ion conduction and the materials, instead, are modest semiconductors. The activation energies, in the range 0.37–0.45 eV, are at the lower end of the values obtained for the best $Li^+$ ion conductors, which again makes it unlikely that these new materials are significant conductors of $Li^+$ ions.

## ACKNOWLEDGMENTS

We thank A. Coats for the EPMA analyses and EPSRC for provision of the EPMA facility.

## REFERENCES

1. J. G. Fletcher, G. C. Mather, A. R. West, M. A. Castellanos, and M. P. Gutierrez, *J. Mater. Chem.* **4,** 1303 (1994).
2. G. C. Mather, R. I. Smith, J. M. S. Skakle, J. G. Fletcher, M. A. Castellanos, M. P. Gutierrez, and A. R. West, *J. Mater. Chem.* **5,** 1177 (1995).
3. J. Hauck, *Acta Crystallogr. Sect. A* **36,** 228 (1980).
4. M. Castellanos and A. R. West, *J. Mater. Sci.* **14,** 450 (1979).